Available online at www.sciencedirect.com
ScienceDirect
Trans. Nonferrous Met. Soc. China 22(2012) 1629−1637
Transactions of Nonferrous Metals Society of China
www.tnmsc.cn

Effects of supersonic fine particles bombarding on thermal barrier coatings after isothermal oxidation

HAN Yu-jun[1,2], YE Fu-xing[1,2], DING Kun-ying[1,3], WANG Zhi-ping[3], LU Guan-xiong[1]

1. Tianjin Key Laboratory of Advanced Joining Technology, School of Materials Science and Engineering, Tianjin University, Tianjin 300072, China;
2. State Key Laboratory of Engines, Tianjin University, Tianjin 300072, China;
3. School of Science, Civil Aviation University of China, Tianjin 300300, China

Received 23 September 2011; accepted 20 December 2011

Abstract: This work was attempted to modify the current technology for thermal barrier coatings (TBCs) by adding an additional step of surface modification, namely, supersonic fine particles bombarding (SFPB) process, on bond coat before applying the topcoat. After isothermal oxidation at 1000 °C for different time, the surface state of the bond coat and its phase transformation were investigated using X-ray diffraction (XRD), scanning electron microscopy (SEM) equipped with energy-dispersive X-ray spectrometry (EDS), transmission electron microscopy (TEM) and Cr^{3+} luminescence spectroscopy. The dislocation density significantly increases after SFPB process, which can generate a large number of diffusion channels in the area of the surface of the bond coat. At the initial stage of isothermal oxidation, the diffusion velocity of Al in the bond coat significantly increases, leading to the formation of a layer of stable α-Al_2O_3 phase. A great number of Cr^{3+} positive ions can diffuse via diffusion channels during the transient state of isothermal oxidation, which can lead to the presence of $(Al_{0.9}Cr_{0.1})_2O_3$ phase and accelerate the $\gamma \rightarrow \theta \rightarrow \alpha$ phase transformation. Cr^{3+} luminescence spectroscopy measurement shows that the residual stress increases at the initial stage of isothermal oxidation and then decreases. The residual stress after isothermal oxidation for 310 h reduces to 0.63 GPa compared with 0.93 GPa after isothermal oxidation for 26 h. In order to prolong the lifespan of TBCs, a layer of continuous, dense and pure α-Al_2O_3 with high oxidation resistance at the interface between topcoat and bond coat can be obtained due to additional SFPB process.

Key words: thermal barrier coatings (TBCs); supersonic fine particles bombarding (SFPB); isothermal oxidation; Cr^{3+} luminescence spectroscopy; dislocation density; diffusion channel

1 Introduction

Thermal barrier coatings(TBCs) are widely used for gas turbine and aero-engine to prevent the superalloy from high temperature corrosion, which can result in an improved component durability to enhance the efficiency of engines, reduce fuel-consumption and prolong the life-span of engines [1−3]. TBCs system usually consists of a MCrAlY-based bond coat on the substrate, a thermally insulating ceramic topcoat deposited by atmospheric plasma spraying (APS) or electron beam physical vapor deposition (EB-PVD) onto bond coat, and a layer of thermally grown oxides (TGO) at the interface between bond coat and topcoat during the thermal exposure [4,5]. Atmospheric plasma spraying (APS), low-pressure plasma spraying (LPPS), vacuum plasma spraying (VPS) and high velocity oxygen-fuel (HVOF) spraying are prevailing deposition facilities of bond coat at present. It is well-established that high efficiency and low cost are the advantages of HVOF process [6−8].

Isothermal oxidation and thermal shock can be considered two fundamental conditions [9,10], which are in accordance with two states-continuous service and abrupt brake in the aero-engine service. The interface between bond coat and topcoat is commonly seen as the most important region for the failure of TBCs [3,5,11]. In particular, the element inter-diffusion may indirectly form TGO after thermal exposure, which is beneficial to the life-span of TBCs [12−15].

In recent years, surface modification for grain refinement has been introduced into improving the

Foundation item: Project (50575220) supported by the National Natural Science Foundation of China; Project supported by State Key Laboratory of Engines, China
Corresponding author: HAN Yu-jun; Tel: +86-22-27406261; Fax: +86-22-27407022; E-mail: hanyujun.nasc@gmail.com; YE Fu-xing; yefx@tju.edu.cn
DOI: 10.1016/S1003-6326(11)61366-6

overall performance by means of modification of surface microstructures [16−18]. As shown in Fig. 1, supersonic fine particles bombarding [19−21] is a new process using supersonic air flow to carry large number of hard solid particles bombarding on metallic surface with high kinetic energy. Additionally, SFPB process can lead to severely plastic deformation grain refinement owing to repetitive bombarding on the metallic surface, consequently metastable microstructure can be formed. The surface microstructure of bond coat tends to become grain refinement, and a large number of dislocations can be generated [22−24]. So far, TBCs deposition using additional SFPB process has been rarely reported. It can be expected that modification of surface microstructure for bond coat has an indirect effect on the phase composition in TGO, as well as the adherence between topcoat and bond coat.

In our work, HVOF process was used to deposit the bond coat, and the surface microstructure of the bond coat was modified subsequently using additional SFPB process, ultimately 8% (mass fraction) yttria-stabilized zirconia (8YSZ) was deposited on the bond coat by APS process.

2 Experimental

The Inconel 718 superalloy (chemical composition is listed in Table 1) discs (*d*25.4 mm×2.5 mm) were used as the substrates, and a grit blasting machine was used to make the substrates rough (pressure 0.8 MPa，sand type 150−180 μm, corundum). Subsequently, a mixture of absolute ethyl alcohol and acetone solution was used to clean the substrates. The NiCoCrAlY powder (Institute of Metal Research, Chinese Academy of Sciences, Shenyang) was taken in a high-velocity fluid fuel oxygen facility (Tafa 5000 system, Praxair Inc., USA) operated with aviation jet fuel and powder carrier gas Ar, selecting oxygen as combustion-supporting gas. For 100 μm-thickness bond coat deposition, a commercially available Tafa Praxair 5000 spraying system was operated with primary gas O_2 and powder carrier gas Ar at 1950 and 12 SCFH, respectively (current 22.7 A, voltage 103 V), with a spray distance of 380 mm in terms of our previous study. The nominal composition of NiCoCrAlY bond coat powders is listed in Table 2. The additional step of SFPB process (74 μm Al_2O_3 powder) instead of grit blasting operated according to the following parameters: 1.3 MPa of the gun pressure, 10 mm of the distance of samples from the SFPB gun, 20 mm/s of lateral velocity, and 13.12 μm of surface roughness in average of the surface of bond coat [22,23]. In order to eliminate the impurities of corundum and expose the surface refinement microstructure of the bond coat, ultrasonic cleaning equipment and electric drying oven with forced convection were conducted. The topcoat was deposited by APS facility (Tafa 3710 system, gun SG−100, Praxair Inc., USA) to produce 200 μm-thickness topcoat using 8YSZ (Al−1075, Praxair Inc., USA) commercial powder. The pressures of primary, secondary and powder carrier gas Ar, H_2 and Ar were selected as 0.4, 0.2 and 0.2 MPa respectively (current 850 A, voltage 37 V), and the spraying distance from the substrate was adjusted to 72 mm. In this study, both HVOF and APS processes were programmed and preformed automatically via the ABB robot. To study the phase transformation of the bond coat after isothermal oxidation, another part of specimens did not deposit topcoat.

The specimens with bond coat were conducted in a high temperature furnace at 1000 °C for 2, 40, 122 and 210 h, respectively, and other specimens with topcoat

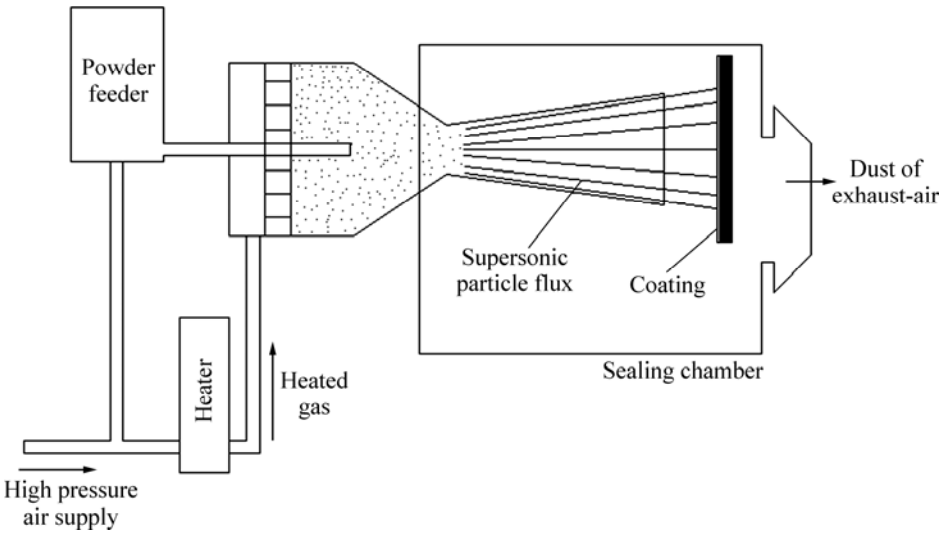

Fig. 1 Schematic diagram of supersonic fine particles bombarding process

were taken out of the furnace after isothermal oxidation for 2, 26 and 310 h respectively and then cooled to the room temperature.

To identify the phase composition of the bond coat after isothermal oxidation, we used a Rigaku Dmax/2500 diffractometer using Cu K_α radiation (DMAX 2500, Rigaku Inc., Tokyo, Japan). The FESEM (S−4800, Hitachi Inc.，Japan), a cold field emission electron microscope equipped with an EDS analyzer (INCA, Oxford Instrument Inc., England), was used to observe the morphology of thermally grown oxides and analyze the elements distribution on the surface of bond coat after isothermal oxidation. Prior to depositing the topcoat, the microstructure of bond coat that has been applied additional SFPB process was also examined, using an instrument of transmission electron microscope (EM−420, Philips, Netherland). Cr^{3+} luminescence spectra were acquired, using a high-performing Renishaw Ramanscope 2000 (Renishaw^{TM}, Gloucestershire, UK) fitted with a motorized mapping stage to measure the frequency shift of alumina in TGO after isothermal oxidation. The laser (He-Ne, 632.8 nm) was focused at 15 positions along flat section of TGO during the measurements and the laser spot size was set as about 1 μm.

Table 1 Nominal composition of Inconel 718 superalloy (mass fraction, %)

Ni	Cr	Mo	Nb	Co	Mn
50−55	17−21	2.8−3.3	4.75−5.5	1	0.35
Si	Cu	Al	Ti	Fe	
0.35	0.3	0.2−0.8	0.7−1.15	Bal.	

Table 2 Chemical composition of NiCoCrAlY powders (mass fraction, %)

Co	Cr	Al	Y	Ni
20.8	17.3	11.5	0.6	Bal.

3 Results and discussion

3.1 Characterization of NiCoCrAlY bond coat after isothermal oxidation

After isothermal oxidation for 40 h, two broad bands at 43.23° and 74.17° with other relatively weak peaks correspond to γ-Ni, γ'-Ni_3Al, β-CoAl, α-Al_2O_3, $(Al_{0.9}Cr_{0.1})_2O_3$, Co_3O_4 and spinel, as shown in Fig. 2. γ-Ni and γ'-Ni_3Al cannot be easily differentiated by XRD patterns due to the same crystal system. It should be noted that the presence of the precipitate γ'-Ni_3Al originating from γ-Ni of {100} crystal plane is in accordance with similar lattice parameter [10]. The presence of a dominant phase represents three strong peaks associated to the atomic planes (100), (200) and (220).

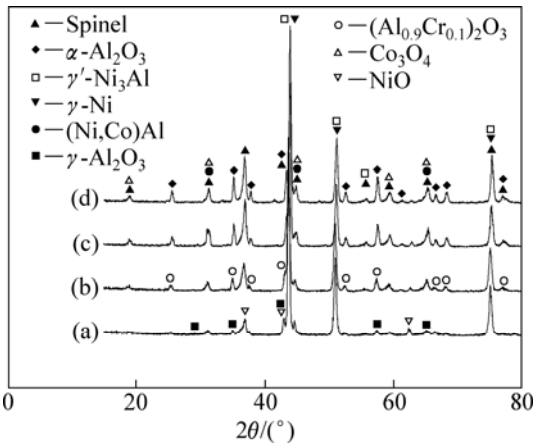

Fig. 2 XRD patterns of bond coat after isothermal oxidation at 1000 °C for different time: (a) 2 h; (b) 40 h; (c) 122 h; (d) 210 h

At the initial stage of isothermal oxidation, a small portion of nickel oxide and oxide of chromium are formed, and then the alumina oxide can be found at the interface between bond coat and topcoat, and a small amount of spinel is formed subsequently due to the chemical reaction [8]. In general, the formation of spinel usually has a negative effects on the stable growth of TGO, thus TBCs are likely to spall in the TGO area. The high growth of spinel can be attributed to aluminum depletion, indirectly leading to the failure of TBCs [25,26]. Therefore, it is critical that the formation of continuous, dense and pure α-Al_2O_3 at the interface between bond coat and topcoat may enhance high temperature corrosion resistance [5]. It should be noted that the initial presence of continuous, dense and pure alumina (γ-Al_2O_3 [monoclinic, P2(3)] and α-Al_2O_3 [rhombohedral, *R*-3*c*(167)]) in TGO can be attributed to the increase of aluminum diffusion rate in bond coat via SFPB process, as shown in Fig. 2(a) and Fig. 3(a). However, a small amount of NiO can also be examined by XRD patterns and SEM (marked in Fig. 3(a) and EDX analysis in Fig. 3(b)) as a result of the reaction diffusion (Ni and O^{2-}). It is expected that the phase composition of TGO mainly consists of α-Al_2O_3 after isothermal oxidation for 122 h.

The metastable γ-Al_2O_3 is formed in the initial 2 h of isothermal oxidation, and then an amount of α-Al_2O_3 can be found when exposed to 1000 °C for 26 h, eventually stable α-Al_2O_3 as the main phase in TGO was obtained. As seen in Fig. 5, the elements distribution of bond coat after 122 h isothermal oxidation was analyzed by EDS map. It can be proven that the surface of oxidized bond coat mainly consists of Al and O, Ni is

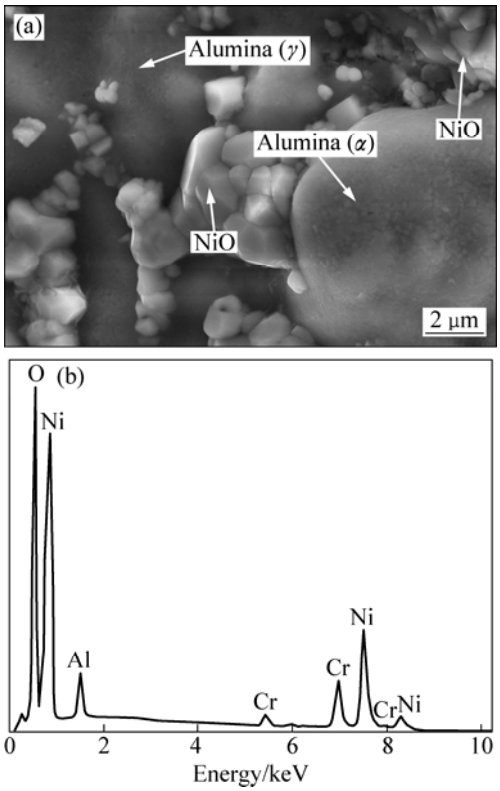

Fig. 3 FESEM image of oxide scale grown on surface of bond coat after isothermal oxidation at 1000 °C for 2 h (a) and EDX analysis of selected area (b)

much less, while Co and Cr show the least amount, which indicates that Al and Ni tend to be selectively oxidized. This result is consistent with the EDX analysis in Fig. 4. Compared with the X-ray diffraction peaks in Fig. 2(a), after isothermal oxidation for 40 h, as shown in Fig. 2(b), β-CoAl, $(Al_{0.9}Cr_{0.1})_2O_3$, Co_3O_4 and spinel phases are formed due to alloy solution and diffusion reaction. The presence of $(Al_{0.9}Cr_{0.1})_2O_3$ phase can be attributed to the fact that a large number of Cr atoms (The radius of Cr atom is larger than that of Al atom) can be substituted for a portion of Al atoms, indirectly leading to the rapid presence of stable α-Al_2O_3.

3.2 Analysis of thermal growth oxides of TBCs

In general, the alumina inclusion phase in TBCs has been under a micro-thermal stress (phase transformation of thermally grown oxide and topcoat) and a macro-stress (thermal mismatch between TGO and YSZ as well as temperature gradient induced thermal stress). Cr^{3+} luminescence spectroscopy (PLPS) can be used to measure the residual stress in TGO, as shown in Fig. 6. The spectrum of unstressed α-Al_2O_3 shows lines R_1 and R_2 (14432 cm^{-1}) from Cr impurity, and the frequency of alumina shifts correspondingly if the alumina was subjected to an uniform stress [27−30]. The frequency shifts of alumina in TGO were measured 15 times, and

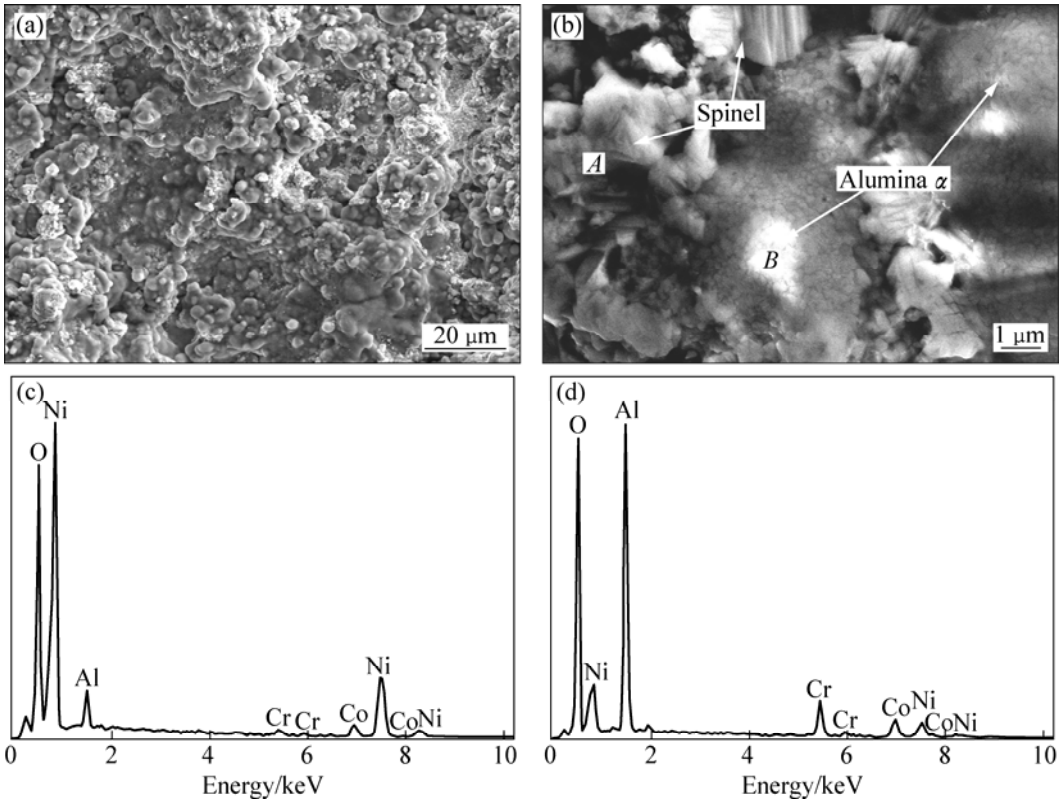

Fig. 4 FESEM images of oxide scale grown on surface of bond coat after isothermal oxidation at 1000 °C for 122 h (a,b) and EDX analysis of two selected areas "*A*" (c) and area "*B*" (d)

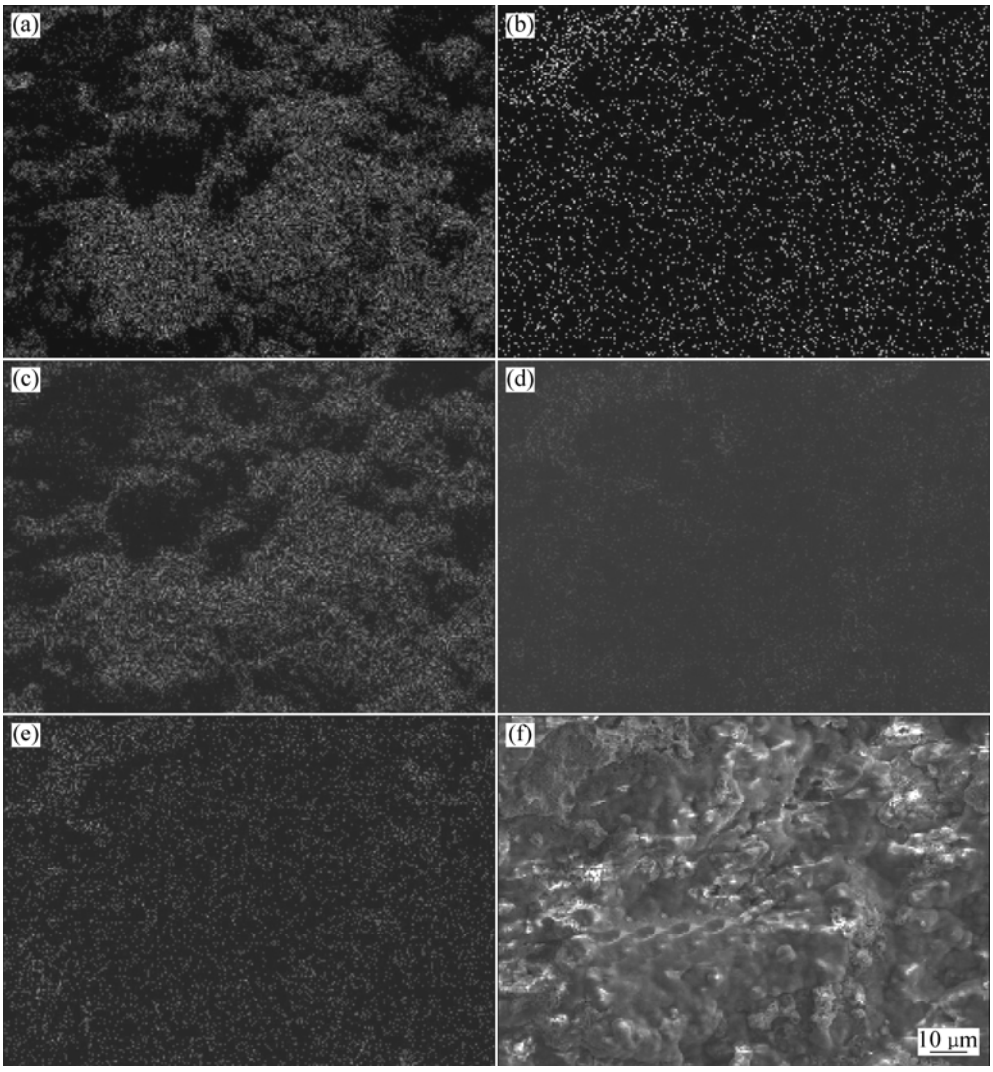

Fig. 5 FESEM image and EDS map resulting from oxides grown on surface of bond coat after isothermal oxidation at 1000 °C for 122 h: (a) EDS map of Al; (b) EDS map of Co; (c) EDS map of O; (d) EDS map of Cr; (e) EDS map of Ni; (f) FESEM image

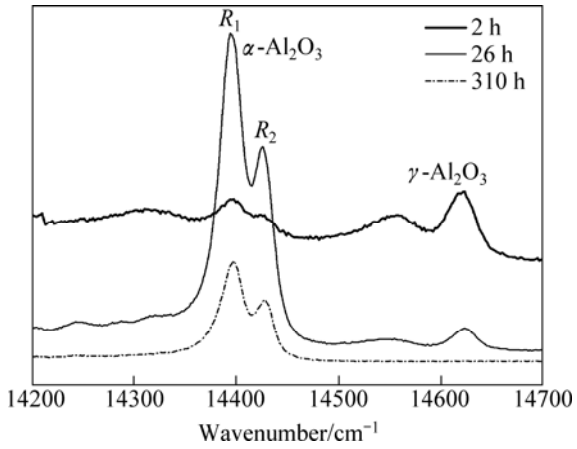

Fig. 6 Typical Cr^{3+} luminescence spectroscopy of TGO in thermal barrier coatings after isothermal oxidation at 1000 °C for 2, 26 and 310 h

the typical results of Cr^{3+} luminescence spectroscopy measurement are illustrated in Fig. 6. In the linear elastic regime, the change in frequency $\Delta\upsilon$ is related to the stress tensor by the following relationship [27,28]:

$$\Delta\upsilon = \Pi_{ij}\sigma_{ij} \quad (1)$$

where $\Delta\upsilon$ is the frequency shift from the stress-free state; Π_{ij} is the piezo-spectroscopic tensor (7.61 cm^{-1}·GPa^{-1}); $\Delta\sigma_{ij}$ is the stress tensor.

The residual stress that is subjected to isothermal oxidation for 310 h is lower than that for 26 h by 0.3 GPa, as shown in Table 3. It can be shown that the residual stress increases at the initial stage of isothermal oxidation and then reduces.

In general, the thermal cycling of TBCs depends heavily on the growth rate of TGO as well as the spinel content except other factors, which will be very likely to spall from the Ni substrate if the thickness of TGO can reach 10 μm approximately [31,32]. As shown in Fig. 7, after 2, 26 and 310 h of isothermal oxidation, the thicknesses of TGO of different specimens reach 1.0, 2.0

Table 3 Summary of thermally growth oxides and phase transformation in TGO measured by photoluminescence piezo-spectroscopy

Time of isothermal oxidation/h	$\Delta\bar{\upsilon}_i$ /cm^{-1}	$\bar{\sigma}$ /GPa	Main elements in TGO	Main phases in TGO
2	−4.4	−0.58	Al, O, Ni, Co	γ-Al_2O_3 (rhombohedral) (46-1212)
26	−7.05	−0.93	Al, O	γ-Al_2O_3, α-Al_2O_3
310	−4.8	−0.63	Al, O	α-Al_2O_3 (monoclinic, P2(3)) (50-1496)

i represents 3 different times of isothermal oxidation, *i*=1, 2, 3.

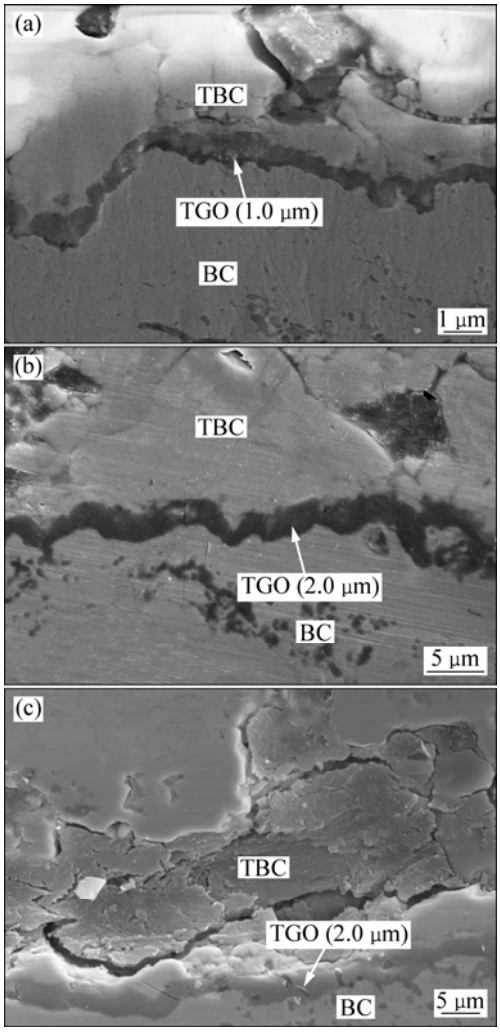

Fig. 7 TGO in thermal barrier coatings after isothermal oxidation at 1000 °C for different time: (a) 2 h; (b) 26 h; (c) 310 h

and 2.0 μm, approximately. The growth kinetics of TGO should be affected by the composition and the surface state of the bond coat. Furthermore, XRD patterns and Cr^{3+} luminescence spectroscopy have clearly confirmed that high growth rate of stable α-Al_2O_3 leading to the retard of spinel growth can have a significant effect on the growth rate of TGO.

The presence of Al_2O_3 originating from the diffusion of Al element and ion O^{2-} from the environment and ceramic topcoat can be found to be in accordance with the concentration peaks of Al and O at the interface between TGO and topcoat, as shown in Fig. 8. It can be investigated that, compared with Al_2O_3, NiO and Co_3O_4 in TGO oxidized for 26 h are far less than in specimens oxidized for 2 h, and the relatively decreased contents of Ni, Co and Cr elements in TGO can show the fact that Al_2O_3 is the main phase in TGO. TOMA et al [7] examined the oxidation process of bond coat isothermally oxidized in air at the temperature ranging from 950 °C to 1200 °C for 2.5, 5, 7.5, 10, 15 and 25 h. After 25 h isothermal oxidation, the main phase of stable α-Al_2O_3 can be detected on the surface of bond coat which is often found to have a carinate-like structure, but only a small quantity of metastable γ-Al_2O_3 or θ-Al_2O_3 was examined. After the HVOF deposition, in our

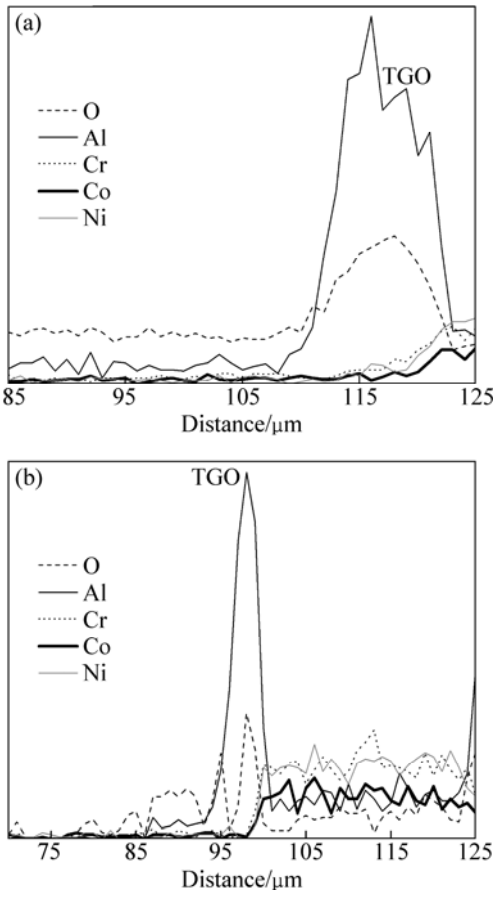

Fig. 8 EDS analysis of TGO in thermal barrier coatings after isothermal oxidation at 1000 °C for 2 h (a) and 26 h (b)

previous study we used SFPB process leading to the surface grain refinement of bond coat, which could generate a large quantity of crystal defects, such as dislocations, twins and stacking faults [22]. It is well established that dissipation and re-combination of dislocations occur when dislocation concentration increase to a certain degree, and the subgrains range from 100 nm to 1000 nm [33] with high deforming stored-energy. From the BF−TEM images of bond coat (applying SFPB process after HVOF deposition) shown in Fig. 9(b), compared with Fig. 9(a), the dislocations in γ-Ni phase providing many diffusion channels can be regarded as the reason that the diffusion velocities of Al, Cr, Co and Ni atoms increase significantly. The physical performance and diffusion behavior of Cr^{3+}, Co^{2+}, Ni^{2+} and Y^{3+} positive ions can play an important part in the thermal stability of alumina. Compared with the radius of Al^{3+}, Cr^{3+} has a similar radius, which results in accelerating the phase transformation of $\gamma\rightarrow\alpha$ after applying SFPB process, leading to the presence of α-Al_2O_3 with close-packed structure [34,35]. As shown in Table 4, metallic oxides such as Al_2O_3 and Cr_2O_3 get the priority to be formed compared with CoO, NiO and Y_2O_3. Furthermore, prior to applying SFPB process, Cr

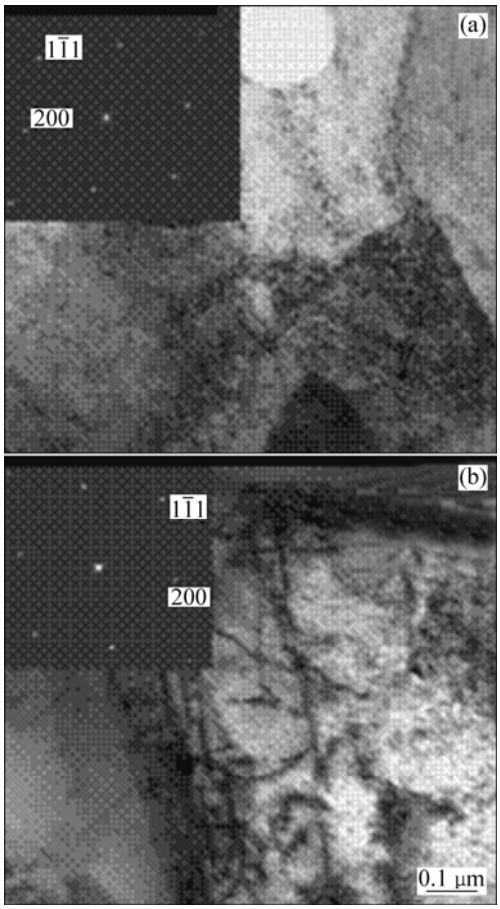

Fig. 9 BF−TEM images of bond coat: (a) HOVF process; (b) SFPB process after HVOF deposition

Table 4 Correlation of standard Gibbs free energy at 1373 K (elements used to NiCoCrAlY bond coat powder)

Element	Al_2O_3	CoO	NiO	Cr_2O_3	Y_2O_3
Standard Gibbs free energy of metallic oxides/ ($kJ\cdot mol^{-1}$)	−1239.1	−135.7	−122.8	−769.6	−106.2

Table 5 Correlation of positive ion radius (elements used to NiCoCrAlY bond coat powder)

Positive ion	Al^{3+}	Co^{2+}	Ni^{2+}	Cr^{3+}	Y^{3+}
Radius/nm	0.050	0.074	0.072	0.052	0.093

atoms have relatively lower diffusion coefficient, which was increased indirectly. As a result, the stage of steady-state of oxidation has been prolonged but the transient state oxidation was decreased, indirectly adjusting and controlling the amount of α-Al_2O_3 in TGO.

4 Conclusions

1) The dislocation density significantly increases after SFPB process, which generates a large number of diffusion channels on the surface of bond coat.

2) At the initial stage of isothermal oxidation, with the increase of aluminum diffusion rate in bond coat via SFPB process, a layer of stable α-Al_2O_3 is formed; however, a small portion of spinel and NiO are formed inevitably due to the reaction diffusion.

3) A great number of Cr^{3+} positive ions can diffuse via diffusion channels during the transient state of isothermal oxidation, leading to the presence of $(Al_{0.9}Cr_{0.1})_2O_3$ phase.

4) The results of Cr^{3+} luminescence spectroscopy show that the residual stress increases at the initial stage of isothermal oxidation and then reduces.

5) After 310 h isothermal oxidation, continuous, dense and pure α-Al_2O_3 can be obtained in TGO.

References

[1] HANCOCK P, MALIK M. Coating systems and technologies for gas turbine applications [C]//COUTSOURADIS D. Materials for Advanced Power Engineering Part 1. Dordrecht: Kluwer Academic Publishers, 1994: 685−704.

[2] WIGREN J，PEJRYD L. Thermal barrier coatings-why, how, where and where to [C]//CODDET C. Proceedings of the 15th ITSC. Ohio, USA: ASM International, Materials Park, 1998: 1531−1542.

[3] EVANS A G, MUMM D R, HUTCHINSON J W, MEIER G H, PETTIT F S. Mechanisms controlling the durability of thermal barrier coatings [J]. Prog Meter Sci, 2001, 46: 505−553.

[4] BOUZAKIS K D, LONTOS A, MICHAILIDIS N, KNOTEK O, LUGSCHEIDER E, BOBZIN K, ETZKORN A. Determination of

mechanical properties of electron beam-physical vapor deposition-thermal barrier coatings (EB-PVD-TBCs) by means of nanoindentation and impact testing [J]. Surf Coat Technol, 2003, 163−164: 75−80.

[5] PADTURE N P, GELL M, JORDAN E H. Thermal barrier coatings for gas-turbine engine applications [J]. Science, 2002, 296: 280−284.

[6] TAYLOR R, BRANDON J R, MORRELL P. Microstructure, composition and property relationships of plasma sprayed thermal barrier coatings [J]. Surf Coat Technol, 1992, 50(2): 141−149.

[7] TOMA D, BRANDL W, KöSTER U. Studies on the transient stage of oxidation of VPS and HVOF sprayed MCrAlY coatings [J]. Surf Coat Technol, 1999, 120−121: 8−15.

[8] CHEN W R, WU X, MARPLE B R, NAGY D R, PATNAIK P C. TGO growth behavior in TBCs with APS and HVOF bond coats [J]. Surf Coat Technol, 2008, 202: 2677−2683.

[9] HAYNES J A, FERBER M K, PORTER W D, RIGNEY E D. Characterization of alumina scales formed during isothermal and cyclic oxidation of plasma-sprayed TBC systems at 1150 °C [J]. Oxid Met, 1999, 52: 31−76.

[10] CHEN He-xing. Study on the diffusion and reaction at the interface of thermal barrier coatings on superalloy substrate [D]. Changsha: Central South University, 2004. (in Chinese)

[11] WRIGHT P K, EVANS A G. Mechanisms governing the performance of thermal barrier coatings [J]. Curr Opin Solid State & Mater Sci, 1999, 4: 255−265.

[12] SOHN Y H, KIM J H, JORDAN E H, GELL M. Thermal cycling of EB-PVD/MCrAlY thermal barrier coatings: Ⅰ. Microstructural development and spallation mechanisms [J]. Surf Coat Technol, 2001, 146−147: 70−78.

[13] TOSCANO J, VAβEN R, GIL A, SUBANOVIC M, NAUMENKO D, QUADAKKERS W J. Parameters affecting TGO growth and adherence on MCrAlY-bond coats for TBCs [J]. Surf Coat Technol, 2006, 201: 3906−3910.

[14] TANG F, SCHOENUNG J M. Local accumulation of thermally grown oxide in plasma-sprayed thermal barrier coatings with rough top-coat/bond-coat interfaces [J]. Scripta Mater, 2005, 52: 905−909.

[15] RABIER A, EVANS A G. Failure mechanisms associated with the thermally grown oxide in plasma-sprayed thermal barrier coatings [J]. Acta Mater, 2000, 48: 3963−3976.

[16] LU K, LU J. Surface nanocrystallizaton(SNC) of metallic materials-presentation of the concept behind a new approach [J]. J Mater Sci Technol, 1999, 15(3): 193−197.

[17] TAO N R, SUI M L，LU J, LU K. Surface nanocrystallization of iron induced by ultrasonic shot peening [J]. Nanostruct Mater, 1999, 11(4): 433−440.

[18] TAO N R, WU X L, SUI M L, LU J, LU K J. Grain refinement at the nanoscale via mechanical twinning and dislocation interaction in a nickel-based alloy [J]. Mater Res, 2004, 19(6): 1623−1629.

[19] XIONG Tian-ying, LIU Zhi-wen, LI Zhi-chao, WU Jie, JIN Hua-zi, LI Tie-fan. Supersonic fine particles bombarding: A novel surface nanocrystallization technology [J]. Material Review, 2003, 17(3): 69−71. (in Chinese)

[20] XIONG Tian-ying, WU Jie, JIN Hua-zi, ZHENG Zong-guang. A method of surface nanocrystallization for metal materials: China, 02109696.1 [P]. 2003−11−26. (in Chinese)

[21] MA G Z, XU B S, WANG H D, SI H J. Effects of surface nanocrystallization pretreatment on low-temperature ion sulfurization behavior of 1Cr18Ni9Ti stainless steel [J]. Appl Surf Sci, 2010, 257: 1204−1210.

[22] ZHANG Li-juan, LIN Xiao-ping, LIU Chun-yang, WANG Zhi-ping, DING Kun-ying, JIA Peng. Effect of high-speed fine particles bombarding on thermally grown oxide growth process of thermal barrier coatings [J]. Transactions of Materials Heat Treatment, 2009, 30(3): 183−186. (in Chinese)

[23] HAN Yu-jun, DONG Yun, WANG Zhi-ping, DING Kun-ying, LIN Xiao-ping, REN Zhi-min. Analysis of residual stress in TGO layer of thermal barrier coatings [J]. Rare Metal Materials and Engineering, 2010, 39(s1): 182−185. (in Chinese)

[24] CHEN Ya-jun, LIN Xiao-ping, WANG Zhi-ping, WANG Li-jun, JI Zhao-hui, DONG Yun. Effects of supersonic fine particles bombarding on thermal cyclic failure lifetime of thermal barrier coating [J]. Harbin Institute of Technology (New Series), 2010, 17(4): 521−526.

[25] YANAR N M, MEIER G H, PETTIT F S. The influence of platinum on the failure of EBPVD YSZ TBCs on NiCoCrAlY bond coats [J]. Scripta Mater, 2002, 46: 325−330.

[26] SHILLINGTON E A G, CLARKE D R. Spalling failure of a thermal barrier coating associated with aluminum depletion in the bond-coat [J]. Acta Mater, 1999, 47(4): 1297−1305.

[27] HE J, CLARKE D R. Determination of the piezo-spectropic coefficients for chromium-doped sapphire [J]. J Am Ceram Soc, 1995, 78: 1347−1353.

[28] MA Q, CLARKE D R. Stress measurement in single-crystal and polycrystalline ceramics using their optical fluorescence [J]. J Am Ceram Soc, 1993, 76(6): 1433−1440.

[29] CHRISTENSEN R J, LIPKIN D M, CLARKE D R, MURPHY K. Non-destructive evaluation of the oxidation stresses through thermal barrier coatings using Cr^{3+}-piezospectroscopy [J]. Appl Phys Lett, 1996, 69(24): 3754−3756.

[30] CLARKE D R, CHRISTENSEN R J, TOLPYGO V. The evolution of oxidation stresses in zirconia thermal barrier coated superalloy leading to oxidation failure [J]. Surf Coat Technol, 1997, 94−95: 89−93.

[31] BRINDLEY W J, MILLER R A. Thermal barrier coating life and isothermal oxidation of low-pressure plasma-sprayed bond coat alloys [J]. Surf Coat Technol, 1990, 43−44: 446−457.

[32] WU B C, CHANG E, CHANG S F, TU D. Degradation mechanism of ZrO_2−8wt%Y_2O_3/Ni−22Cr−10Al−1Y thermal barrier coatings [J]. J Am Ceram Soc, 1989, 72(2): 212−218.

[33] YONG X P, LIU G, LU J, LU K. Fabrication and characterization of nanostructured surface of low carbon steel [J]. Acta Metallurgica Sinica, 2002, 38: 157−160. (in Chinese)

[34] BURTIN P, BRUNELLE J P, SOUSTELLE M. Influence of surface area and additives on the thermal stability of transition alumina catalyst. Supports Ⅰ: Kinetic data [J]. Appl Catal, 1987, 34: 225−238.

[35] BURTIN P, BRUNELLE J P, PIJOLAT M, SOUSTELLE M. Influence of surface area and additives on the thermal stability of transition alumina catalyst. Supports Ⅱ: Kinetic model and interpretation [J]. Appl Catal, 1987, 34: 239−254.

超音速微粒轰击对热障涂层高温氧化行为的影响

韩玉君[1,2]，叶福兴[1,2]，丁坤英[1,3]，王志平[3]，陆冠雄[1]

1. 天津大学 材料科学与工程学院，天津市现代连接技术重点实验室，天津 300072；
2. 天津大学 内燃机燃烧学国家重点实验室，天津 300072；
3. 中国民航大学 理学院，天津 300300

摘 要：在传统的热障涂层(TBCs)制备工艺的基础上，在制备热障涂层陶瓷层前，采用超音速微粒轰击技术(SFPB)改变粘结层的表面状态。采用 X 射线衍射分析仪(XRD)、扫描电子显微镜(SEM)、能谱仪(EDS)、透射电子显微镜(TEM)和微区 Cr^{3+}荧光光谱研究粘结层的表面结构及其 1000 ℃ 时的高温氧化相变。粘结层表面位错密度大幅度增加，形成了大量的原子扩散通道；在高温氧化初期，粘结层中 Al 原子扩散速度的增快保证了优先形成一层稳定的 α-Al_2O_3 相；在高温氧化瞬态阶段，大量 Cr^{3+}通过 SFPB 产生的扩散通道，形成过渡相$(Al_{0.9}Cr_{0.1})_2O_3$，该过渡相间接促进了 $\gamma\rightarrow\theta\rightarrow\alpha$ 相变。在高温氧化初期，热障涂层 TGO 中的残余应力先急剧增大然后减小；与高温氧化 26 h 的 0.93 GPa 相比，高温氧化 310 h 的残余应力降低至 0.63 GPa。在热障涂层的 TGO 层中获得了单一、连续、致密的具有抗高温氧化能力的主相 α-Al_2O_3，这利于进一步延长其使用寿命。

关键词：热障涂层(TBCs)；超音速微粒轰击(SFPB)；高温氧化；Cr^{3+}荧光光谱；位错密度；扩散通道

(Edited by YANG Hua)